Study of the Compositional Changes of Mango during Ripening by Use of Nuclear Magnetic Resonance Spectroscopy

Ana M. Gil,*,† Iola F. Duarte,† Ivonne Delgadillo,† Ian J. Colquhoun,‡ Francesco Casuscelli,‡ Eberhard Humpfer,§ and Manfred Spraul§

Department of Chemistry, University of Aveiro, 3810 Aveiro, Portugal; Institute of Food Research, Norwich Laboratory, Norwich Research Park, Colney, Norwich NR4 7UA, U.K.; and Bruker Analytiche Messtechnik GmbH, Silberstreifen, D76287-Rheinstetten, Germany

Liquid-state NMR spectroscopy was used to follow the compositional changes in mango juice during ripening, whereas MAS and HR-MAS techniques enabled resolved ^{13}C and ^{1}H NMR spectra of mango pulps to be recorded. Spectral assignment enabled the identification of several organic acids, amino acids, and other minor components, and the compositional changes upon ripening were followed through the changes in the spectra. In pulps, sucrose was found to predominate over fructose and glucose at most ripening stages, and citric acid content decreased markedly after the initial ripening stages while alanine increased significantly. Other spectral changes reflect the complex biochemistry of mango ripening and enabled the role played by some compounds to be discussed. Some differences observed between the composition of juices and pulps are discussed. This work shows that NMR spectroscopy enables the direct characterization of intact mango pulps, thus allowing the noninvasive study of the overall biochemistry in the whole fruit.

Keywords: *^{1}H NMR; MAS; mango fruit; juice; ripening*

INTRODUCTION

Mango fruit (*Mangifera indica* L.) is one of the most important commercial fruit crops, being the second largest tropical crop next to banana, in terms of production, acreage, and popularity (Salunkhe and Desai, 1984). The trade of mango has been, however, somewhat limited by significant postharvest wastage due to the highly perishable nature of this fruit. To be able to control postharvest quality and develop appropriate technologies to enhance the marketable lifetime of the mango, comprehensive knowledge of its chemical composition and biochemical changes upon ripening and rotting is required.

Mango chemical composition has been the subject of several studies primarily dedicated to the identification of sugars and organic acids (Medlicott and Thompson, 1984; Medlicott et al., 1986; Selvaraj et al., 1989; Castrillo et al., 1992; Ito et al., 1997) and with increasing interest in minor fractions such as cell wall components (Tucker and Seymour, 1991; Mitcham and Mcdonald, 1992; Aina and Oladunjoye, 1993; Muda et al., 1995; Ollé et al., 1996), carotenoids (Sudhakar and Maini, 1994; Cano and Ancos, 1994; Wilberg and Rodriguez-Amaya, 1995; Mercadante et al., 1997; Mercadante and Rodriguez-Amaya, 1998), and volatile compounds (Engel and Tressl, 1983; Koulibaly et al., 1992; Chassagne and Crouzet, 1995; Malundo et al., 1997; Sakho et al., 1997; Ollé et al., 1998). Many of these studies have shown that the changes in chemical composition during mango ripening are strongly dependent on cultivar, climate, stage of maturity at harvest, and conditions of postharvest storage. The studies of sugar and organic acid compositions (Medlicott and Thompson, 1984; Medlicott et al., 1986; Selvaraj et al., 1989; Castrillo et al., 1992; Ito et al., 1997) have indicated that total sugars increase and acidity decreases as ripening proceeds. In addition, the compositional changes with ripening of the carotenoids fraction (Sudhakar and Maini, 1994; Mercadante and Rodriguez-Amaya, 1998) and of mango cell walls (Tucker and Seymour, 1991; Mitcham and Mcdonald, 1992; Aina and Oladunjoye, 1993; Muda et al., 1995) have also been characterized.

Most studies have involved separation of the liquid phase of the fruit, followed by analysis by chromatographic methods, particularly high-performance-liquid-chromatography (HPLC). However, the extent to which the invasive separation and fractionation methods may interfere with the biochemistry of the fruit is not known. Therefore, the demand for noninvasive methods of fruit analysis has increased significantly, and some recent studies have used a number of noninvasive techniques such as microscopy (Usha et al., 1997), X-ray imaging (Thomas et al., 1993), ultrasonics (Mizrach et al., 1997), and spectroscopy (Joyce et al., 1993; Usha et al., 1994; Bhushan et al., 1994; Bustos et al., 1996; Guthrie and Walsh, 1997) to evaluate mango quality. Nuclear magnetic resonance (NMR) spectroscopy has played an increasingly important role in the compositional study of foods (Eads and Bryant, 1986; Ni and Eads, 1992, 1993a,b; Gil et al., 1996; Belton et al., 1996, 1997), particularly fruit juices (Eads and Bryant, 1986; Belton et al., 1996, 1997). Magic angle spinning (MAS) NMR has also been used to characterize the composition of

* To whom correspondence should be addressed. Tel: +351 234 370 707, fax: +351 234 370 084, e-mail: agil@dq.ua.pt.
† University of Aveiro.
‡ Institute of Food Research.
§ Bruker Analytiche Messtechnik GmbH.

10.1021/jf9911287 CCC: $19.00
Published on Web 04/01/2000

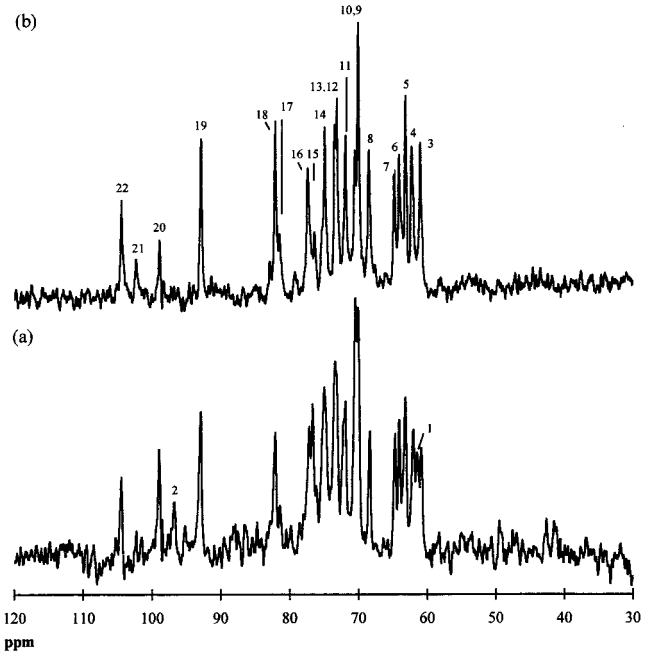

Figure 1. Standard ^{13}C MAS NMR spectra of (a) mango pulp of day 1 and (b) mango pulp of day 9. Spinning rate used was 1200 Hz. The assignment of the peaks numbered is as follows (F: fructose, G: glucose, S: sucrose): 1- G (C_6); 2- G ($C_{1\beta}$); 3- S (C_6, glucose ring); 4- S (C_1, fructose ring); 5- S (C_6, fructose ring); 6- F ($C_{6\beta p}$); 7- F ($C_{1\beta p}$); 8- F ($C_{5\beta p}$); 9,10- S (C_4, glucose ring) + G ($C_{5\alpha p}$ or $C_{5\beta p}$) + F ($C_{4\beta p}$, $C_{3\beta p}$); 11- S (C_2, glucose ring); 12- S (C_5, glucose ring); 13- S (C_3, glucose ring); 14- S (C_4, fructose ring); 15- G ($C_{5\alpha p}$ or $C_{5\beta p}$); 16- S (C_3, fructose ring); 17- F ($C_{3\alpha f}$);18- S (C_5, fructose ring); 19- S (C_1, glucose ring); 20- F ($C_{2\beta p}$); 21- F ($C_{2\beta f}$); 22- S (C_2, fructose ring).

some fruits by direct study of the pulps (Ni and Eads, 1992, 1993a,b), thus avoiding the use of extraction and separation methods. Recent instrumental developments in MAS NMR equipment have enabled the use of high-resolution MAS (HR-MAS) NMR leading to a significant resolution improvement in the spectra of solid or semisolid food samples (Gil et al., 1997) so that components other than the main sugars may become detectable in intact fruits.

The results reported here describe the use of solid state and liquid-state NMR spectroscopy to follow the compositional changes, during ripening, in intact mango and in mango juice, respectively. We aim to show that HR-MAS NMR spectroscopy is a suitable nondestructive analytical tool for fruit analysis, enabling characterization of fruit composition without requiring separation or extraction steps.

MATERIALS AND METHODS

Materials. The mango fruits studied were of the "Tommy Atkins" cultivar and were obtained commercially at the same initial ripening stage as evaluated by color and firmness. The fruits were left to ripen at 23 °C until clear differences in their appearance were observed. Hence, the following ripening stages were identified and described in terms of the number of days counted after the selection of the fruits: day 1 − high firmness, green-colored skin and light yellow pulp; day 5 − slightly softer texture, green skin with some yellow spots and yellow pulp; day 9 − soft texture, green-yellow skin and intensely yellow pulp; day 15 − very soft texture, yellow-orange skin and intensely yellow pulp; day 19 − all the latter properties as well as a slight reddish coloring of the skin. On each of these days, pulp samples were collected from the equatorial ring of the fruit, and juice samples were obtained

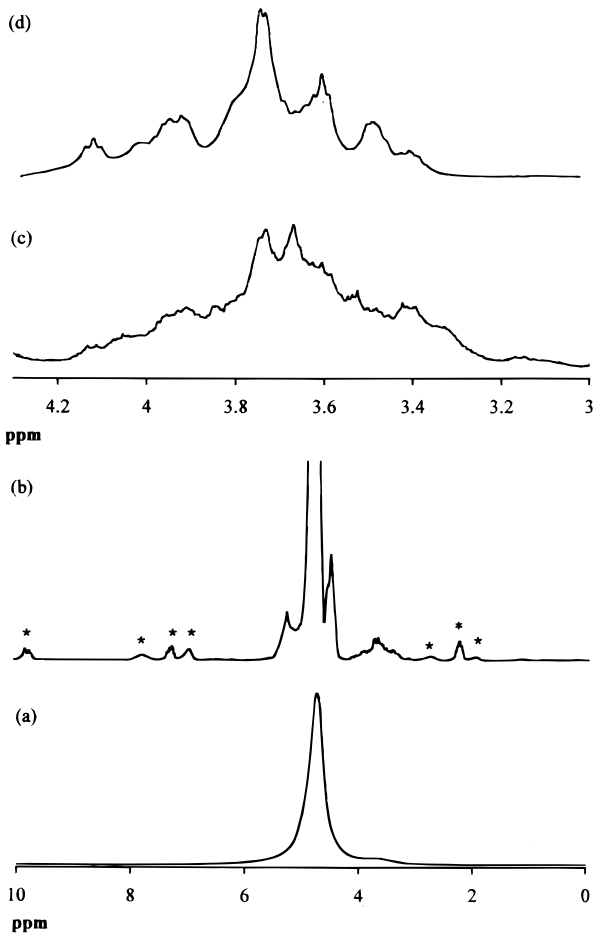

Figure 2. Standard ^1H NMR spectra of mango pulps: (a) static ^1H NMR spectrum of mango pulp of day 1, (b and c) ^1H MAS NMR spectrum of mango pulp of day 1, (d) ^1H MAS NMR spectrum of mango pulp of day 9. Spinning rate used was 1200 Hz. *: spinning sidebands.

by filtration of the macerated pulp. Pulps and juices were stored at −20 °C until their study by NMR. The juice of day 5 could not be collected so that only the remaining juice samples will be considered in the following discussion. For the ^1H HR-MAS NMR of pulps, the samples were mixed with 2−3 drops of D_2O containing sodium 3-(trimethylsilyl)propionate-d_4 (TSP-d_4, chemical shift reference) and packed into a 4 mm MAS rotor. For solution state NMR, D_2O containing TSP was added to the juices to give samples with 10% D_2O and 0.01% TSP.

NMR Spectroscopy. The standard ^1H and ^{13}C MAS NMR spectra of mango pulps were recorded on a Bruker MSL 400P spectrometer, operating at 400 MHz (^1H) or 100 MHz (^{13}C) and using a standard double bearing MAS probe and rotor. Samples were spun at 1.2 kHz and a 90° pulse length of 4−5 μs was used, together with a 3−5 s recycle delay. The HR-MAS spectra of pulps were recorded on a Bruker Avance DRX-400 spectrometer operating at 400 MHz for ^1H. A 4 mm HR-MAS probe was used together with an MAS rotor containing two hemispherical Teflon inserts. The samples were spun at 4.3−4.5 kHz, and a 13 μs 90° pulse was used together with a 1.5 s recycle. All 1D spectra were acquired with presaturation of the water peak. The effect of sample spinning on the pulp spectra was investigated by comparing the 1D spectra recorded before and after a period of a few hours. No significant spectral changes were observed, thus suggesting that spinning at about 4 kHz, during 3−4 h, does not physically damage the sample. Total correlation NMR spectra (TOCSY), $^1H/^{13}C$ correlation NMR spectra, and *J*-resolved NMR spectra were obtained for the pulps of day 1 and day 19. The $^1H/^{13}C$ correlation spectra were obtained with SW of 5000 Hz and 72000 Hz in the proton and carbon dimensions, respectively, 1 K data points, 40 scans,

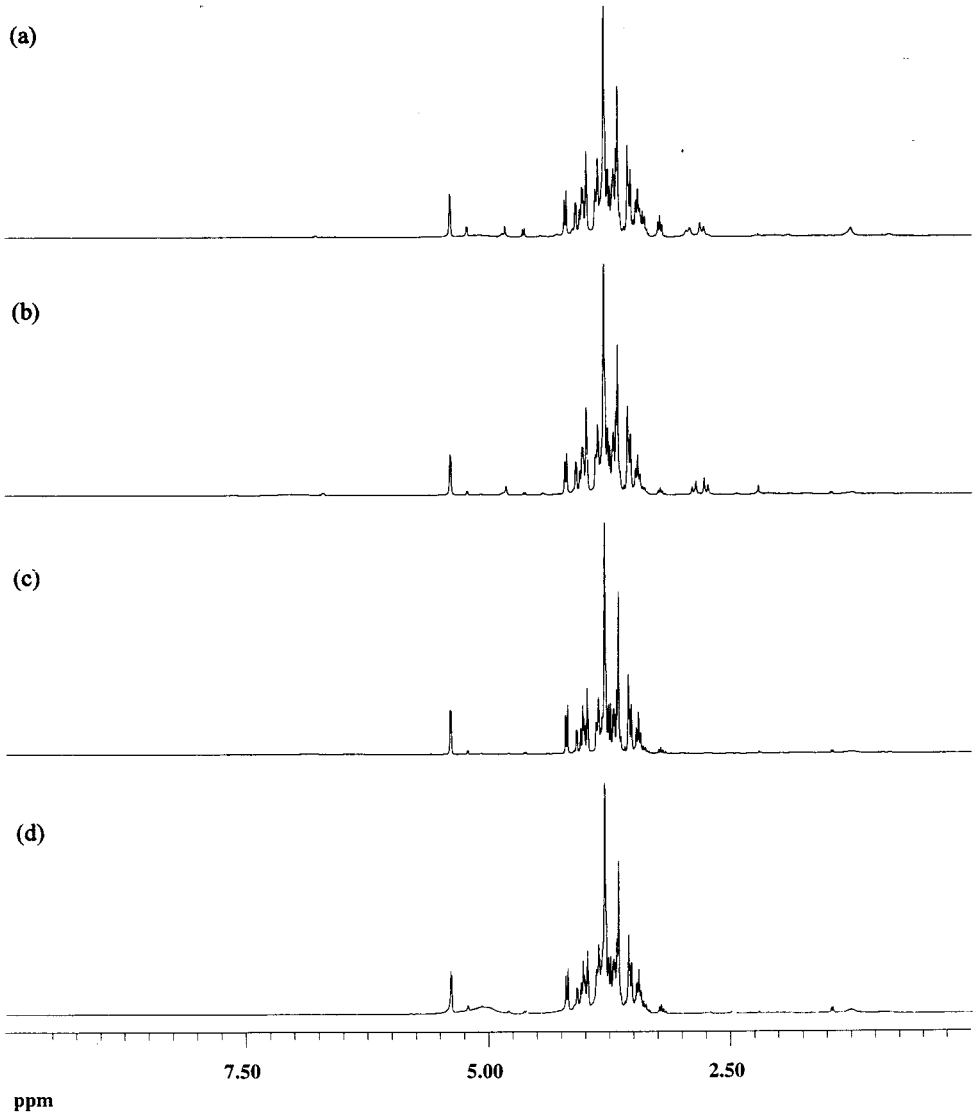

Figure 3. ^{1}H HR-MAS NMR spectra of mango pulps of (a) day 1, (b) day 5, (c) day 15 and (d) day 19. Spinning rate used was 1200 Hz for all spectra.

200 increments and a recycle time of 2 s. The TOCSY spectra were acquired with SW of 6400 Hz in both dimensions, 2K data points, 8 scans in the F2 dimension, 200 increments, and a mixing time of 20 ms. The *J*-resolved spectra were acquired with SW of 10000 Hz in the proton dimension and 78 Hz in the *J* dimension. 8K data points were acquired with 8 scans for each of 64 increments.

The NMR spectra of the juice samples were acquired on a Bruker DRX-600 spectrometer, operating at a 600 MHz frequency for ^{1}H. The 1D spectra were obtained with presaturation of the water peak, with a 7.9 μs 90° pulse and a 2.2 s recycle delay. ^{1}H/^{13}C correlation NMR spectra were acquired with SW of 10000 Hz and 99600 Hz in the proton and carbon dimensions, respectively, with 2K data points, 48 scans, and 300 increments. The correlation spectroscopy (COSY) experiment was acquired with SW 10000 Hz in both dimensions, 4K data points, 16 scans, and 200 increments.

RESULTS AND DISCUSSION

Standard ^{13}C and ^{1}H MAS NMR of Mango Pulps. Figure 1a shows the ^{13}C MAS NMR spectrum of unripe mango pulp obtained for the day 1 sample. The spectrum of the same sample recorded under nonspinning conditions (not shown) showed very low signal-to-noise ratio due to considerable line-broadening. This broadening arises from anisotropic magnetic susceptibility effects in the pulp medium (Ni and Eads, 1992; Belton and Gil, 1996) which may be averaged out by MAS at a rate comparable to the strength of the line-broadening mechanism. Magnetic susceptibility effects typically amount to a few hundred hertz and, indeed, spinning the mango sample at relatively low rates (1200 Hz) results in a marked increase of spectral resolution, allowing the spectrum shown in Figure 1a to be recorded. The same figure also shows the spectrum obtained for the pulp of day 9 (Figure 1b). The assignment of the ^{13}C NMR spectra was carried out by comparison with chemical shifts observed for single sugar solutions, showing that all peaks observed arise from the three main sugars found in mango: sucrose, glucose, and fructose. One of the changes in the ^{13}C NMR spectra as the fruit ripens from day 1 to day 9 is a very slight resolution improvement, expected on the basis that as the pulp becomes softer the correlation times of most compounds become shorter. In addition, signals 1 and 2 in Figure 1a, assigned to Glc C_6 and $C_{1\beta}$, disappear in Figure 1b, indicating a significant decrease in glucose content between days 1 and 9, relative to the remaining sugars. On the other hand,

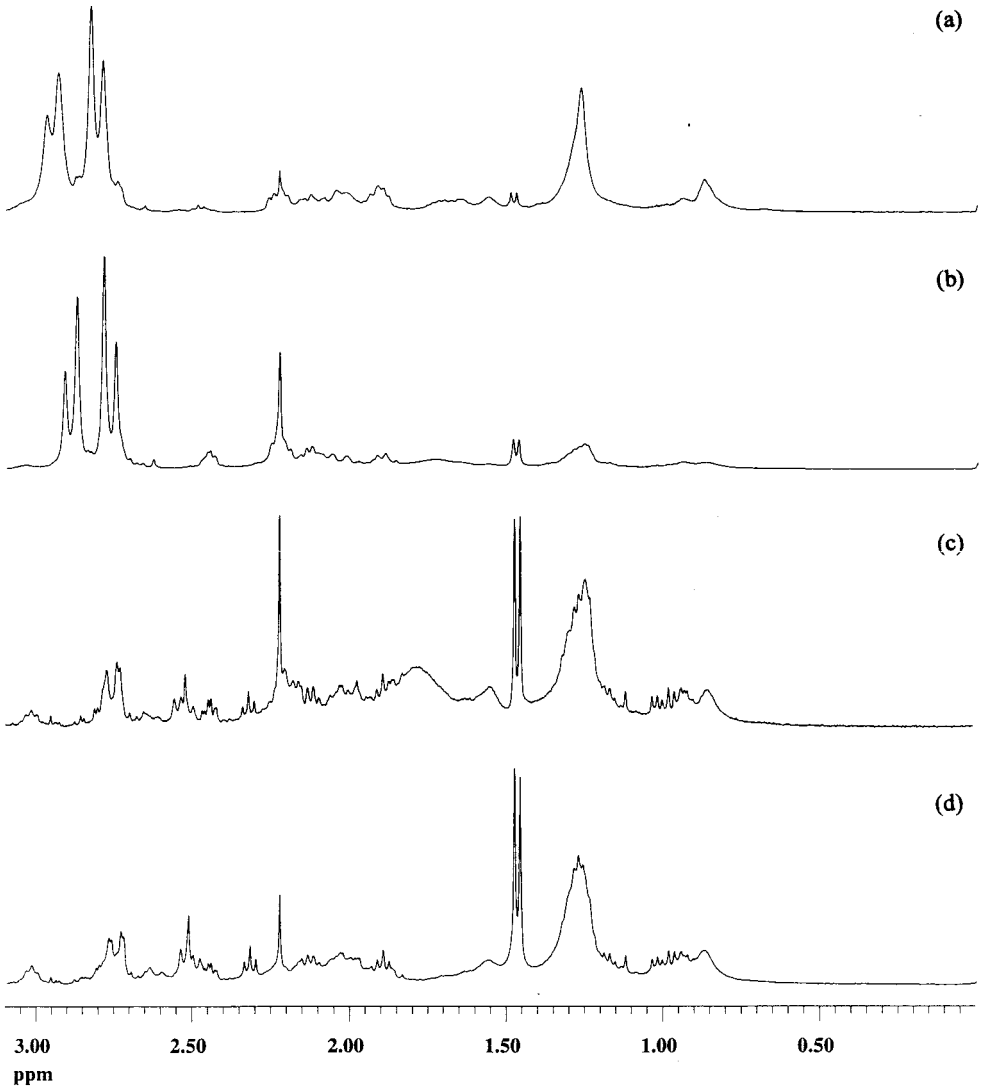

Figure 4. Expansions of the 0−3.0 ppm regions of the spectra shown in Figure 3.

the relative content of sucrose increases in the same period, as shown by the increase of peaks 5 and 18. However, limited information is provided by the ^{13}C MAS NMR spectra about the overall biochemistry of the ripening mango since no peaks from nonsugar components could be identified. ^{1}H NMR, with its greater sensitivity, may stand a better chance of enabling the detection of metabolites other than sugars in fruit pulps, provided that sufficient line-narrowing can be achieved.

Standard MAS also results in significant resolution improvement in the ^{1}H NMR spectra of mango pulp (Figure 2a,b) but, again, only sugar resonances may be easily observed, in the 3.0−4.2 ppm region and at about 5.2 ppm (Figure 2b). The same spectrum also shows an intense signal at 4.48 ppm, probably arising from HOD. However, the resolution achieved in the ^{1}H MAS spectrum, with sample spinning of 1200 Hz, is still not high enough to enable objective assignments of the sugar peaks to be made or efficient water suppression techniques to be employed. Ripening seems to lead to changes affecting the sugar region of the ^{1}H spectra (Figure 2c,d), but the insufficient spectral resolution impedes further study of those changes.

^{1}H HR-MAS NMR of Mango Pulps. Using an HR-MAS probe, the spectral resolution of the ^{1}H spectrum is very significantly improved (Figures 3−6) compared to standard MAS (Figure 2). Furthermore, the resolution achieved under such conditions enables efficient presaturation of the water peak (Figure 5) as well as the recording of 2D NMR spectra of the fruit pulp. The NMR spectra of the corresponding juices (Figures 7−9) still present higher resolution than those of the pulps, due to both the shorter correlation times of compounds in the liquid phase and the use of a higher field strength to record the juice spectra. The changes observed in the different regions of the 1D spectra of pulps (Figures 4−6) and juices (Figures 7−9) clearly demonstrate that significant compositional changes take place as the mango ripens. Before studying these changes, spectral assignment was carried out based on the 1D and 2D spectra of the juices and pulps. Figure 10 shows part of the TOCSY spectrum of day 19 pulp. *J*-resolved and $^{1}H/^{13}C$ correlation spectra were also recorded for mango pulps (not shown) and used for spectral assignment, together with the aid of chemical shifts and coupling constants of compounds found in the literature (Nicholson et al., 1995; Fan, 1996; Colquhoun, 1998).

Spectral Assignments: Juices and Pulps. The assignments are presented in Table 1, and selected ones are discussed below. The spectrum obtained for day 15 (Figures 7b, 8b, and 9b) shows most of the peaks identified so that, unless otherwise stated, the assign-

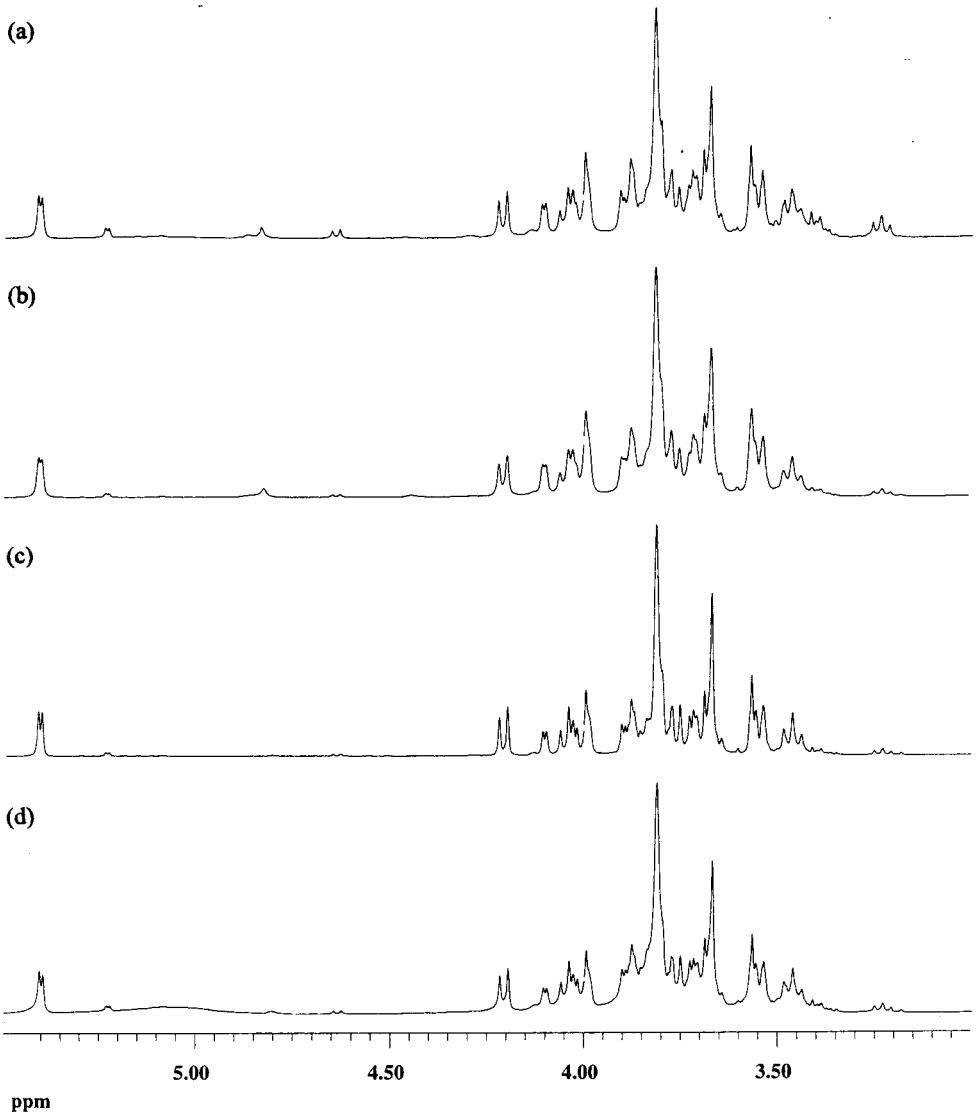

Figure 5. Expansions of the 3.0−5.5 ppm regions of the spectra shown in Figure 3.

ments in Table 1 refer to day 15. As expected, sucrose, glucose, and fructose are seen in all ^{1}H NMR spectra as being the major components of the fruit. However, many other compounds may be detected from signals in the nonsugar regions of the spectra.

High-Field Region (0−3.0 ppm, Figures 4 and 7). Generally, this region shows signals arising from aliphatic groups of organic acids and amino acids as well as from ethanol (Table 1). A group of several overlapped doublets is visible at 1.25−1.28 ppm, with cross-peaks (COSY) at ∼3.8 ppm and H/C correlations to ∼17.4 ppm (^{13}C). One possible assignment of these bands is to sugars' Me groups (rhamnose, fucose) derived from cell wall polysaccharides. In the HR-MAS spectra (Figure 4) a series of broad bands appear, of which the most prominent is at 1.28 ppm. The correlations of the 1.28 ppm peak to signals at 0.85, 1.56, 2.02, and 2.22 ppm in the TOCSY spectrum of pulp (Figure 10), together with its correlation to a ^{13}C signal at 29.5 ppm (not shown), strongly suggest an assignment to methylene groups belonging to the lipids fraction present in mango. A second set of correlated peaks in the TOCSY spectrum of the pulps (2.02, 2.75, 5.30 ppm) is consistent with the presence of unsaturated lipid chains. It is interesting to note that this set of peaks is not identified in the juice spectra, thus showing, as expected, that these lipids are not located in the aqueous phase in large amounts. Within the many compounds identified in the 1.33−3.0 ppm region, there are several organic acids (Table 1). The chemical shifts indicated for these acids refer to the samples collected at day 15, and it should be noted that, because of their dependence on pH, those chemical shifts will be different for samples at other ripening stages. The singlet at 2.53 ppm may arise from succinic acid and/or from methylamine, and the singlet at 2.01 ppm observed in the juice spectrum of day 19 (Figure 7c) remains unassigned. This peak may arise from a methyl group, either of acetate ion or of an acetate-derived ester. The assignment to an acetate ester is particularly probable since a number of those compounds have been reported in the volatile fraction of mango (Engel and Tressl, 1983). The strong singlet at 2.20 ppm in the spectra of pulp and juice of day 1 (Figures 4a and 7a) also remains, at this stage, unassigned.

Mid-Field Region (3.0−5.5 ppm, Figures 5 and 8). In this region, the main contributions arise from the three principal sugars and overlapped contributions from amino acids, organic acids, ethanol, and methanol (Table 1). Other peaks may arise from cell wall sugars: β-fucose (3.78 ppm), β-rhamnose (3.88 ppm), β-galactose

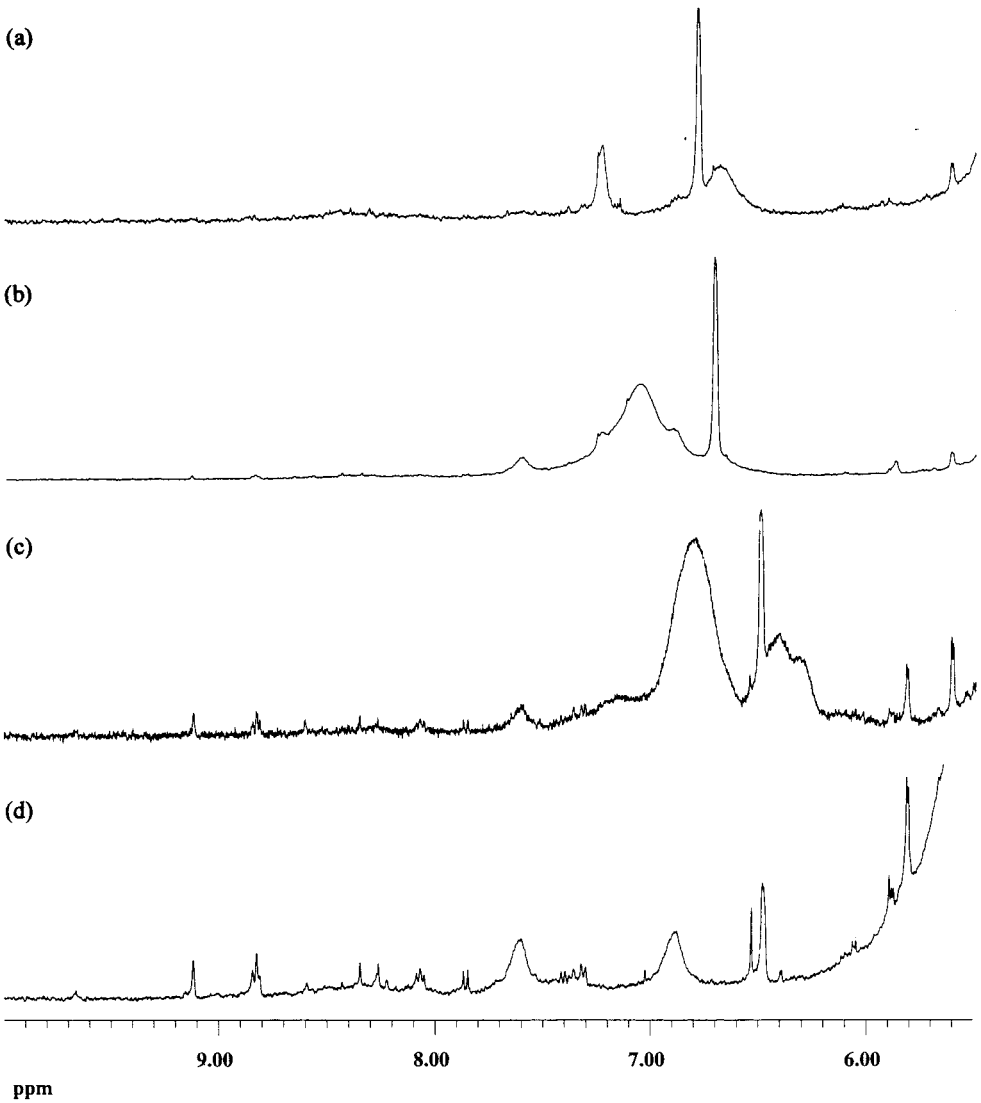

Figure 6. Expansions of the 5.5−10.0 ppm regions of the spectra shown in Figure 3.

(3.49 and 4.57 ppm). The main difference between the spectra of pulps and juices in the 3.0−5.5 ppm region relates to the lower intensity in the spectra of pulps of the glucose peaks relative to those of sucrose (Figures 5d and 8b). This observation suggests that different sugar proportions may characterize the liquid phase and the intact mango fruit. This point will be discussed later.

Low-Field Region (5.5−10 ppm, Figures 6 and 9). The signals situated in this region are the weakest in the spectra and arise from aromatic groups of amino acids and phenolic compounds. Partial assignment of these peaks was achieved and, besides the several organic acids identified (Table 1), the two broad resonances seen at 6.88 and 7.61 ppm at day 19 (Figures 6d and 9c) are suggested to arise from polyphenolic compounds, similarly to those reported previously in apple juices (Belton et al., 1997; Colquhoun, 1998).

Spectral Changes during Ripening. On the basis of the assignments made, the following discussion will concern the changes taking place in the spectra of mango pulps and mango juices during ripening. Due to the difficulty in using an intensity reference peak in the solid phase, only qualitative and semiquantitative considerations will be made at this stage, based on relative intensity changes. In the discussion that follows, changes in the major components (sugars, citric acid) will be discussed first, followed by changes in the less-abundant metabolites.

Sugars. The ^{1}H HR-MAS spectra of mango pulps (Figures 4 and 5) show that the main components of day 1 (unripe) mango are the sugars (glucose, fructose, and sucrose) and citric acid, in agreement with previous reports on the composition of mango of the "Tommy Atkins" variety (Medlicott et al., 1984). By integrating the sucrose anomeric peak at 5.40 ppm, the α-glucose anomeric peak at 5.23 ppm and the β-glucose H2 triplet at 3.25 ppm, the spectral areas contributed by each of the three sugars could be estimated by multiplying the single peak areas by the total number of protons in each sugar. In the case of β-glucose, the integral of the H2 multiplet was considered instead of the anomeric one at 4.64 ppm. The integrated intensity of the latter is reduced due to its proximity to the saturated water resonance. For fructose, the only peak relatively free of overlap is the 4.11 ppm peak arising from H3 and H4 of the β-furanose form. This is, however, a poor indication of the spectral contribution of fructose since the β-pyranose form is expected to occur in higher abundance, in aqueous solution: 65% β-pyranose and 25% β-furanose, at 31 °C (Angyal, 1984). Therefore, the

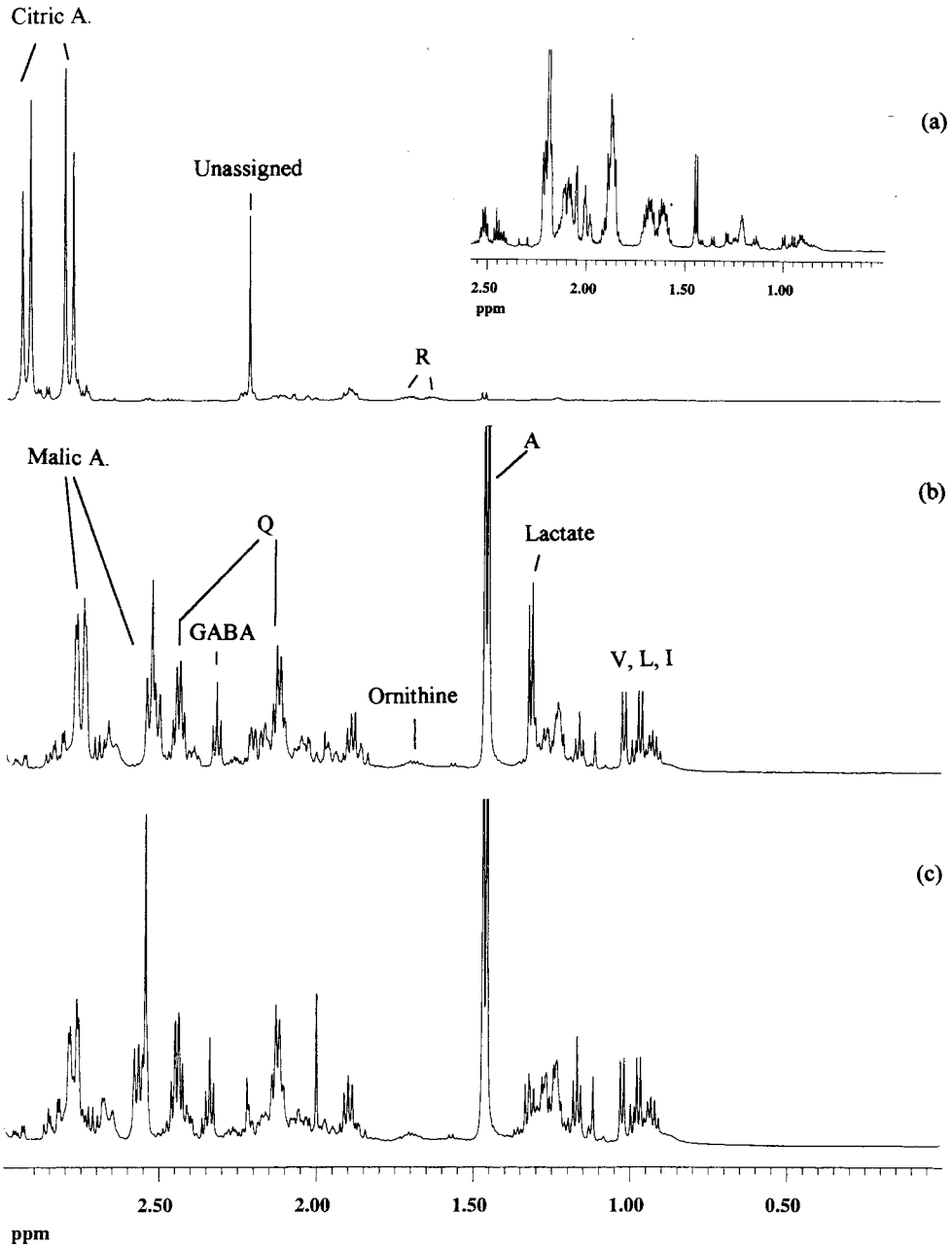

Figure 7. Expansions of the 0−3.0 ppm regions of the 1D ^{1}H NMR spectra of juices of (a) day 1, (b) day 15, and (c) day 19. Standard single letter abbreviations are used for amino acids.

fructose contribution was obtained by subtracting the glucose and sucrose contributions from the measured total area in the spectral sugar region. This total area is a satisfactory approximation of the total sugar content since the contribution of minor components was found to be very small by comparing the actual spectra with those of the individual main sugars.

Table 2 shows the percentages of each sugar estimated on the basis of the NMR spectra of pulps and juices. The data obtained for the pulps from HR-MAS spectra will be discussed first, followed by that for the corresponding juices from conventional high resolution NMR. For the pulp of day 1, the sugar molar composition is 20.4% glucose, 38.2% fructose, and 41.3% sucrose. This is in broad agreement with the relative amounts reported previously for "Tommy Atkins" mango after 3 days of ripening: 15.5% glucose, 27.5% fructose, and 57.1% sucrose (Table 2), but the differences between the percentages for each sugar should be noted. Such differences between the results reported here and those found in the literature may be related to the subjectivity in defining the ripening stage of the fruit, particularly within different laboratories. Furthermore, any differences between the intact fruit and the juices may also reflect real compositional differences between the intact fruit and its liquid phase. The results shown in Table 2 for the pulps show that the percentage of sucrose increases 1.3-fold from day 1 to day 19 which is in very good agreement with the 1.3-fold increase reported in the literature for the juice. The percentage of fructose in mango pulp shows an initial increase from day 1 to day 5, followed by a decrease back to a value close to the initial one. Again, this variation is in close agreement with the one expected in view of previous work. Finally, the total glucose percentage of 20% for day 1 decreases 3-fold until day 15. The apparent increase at

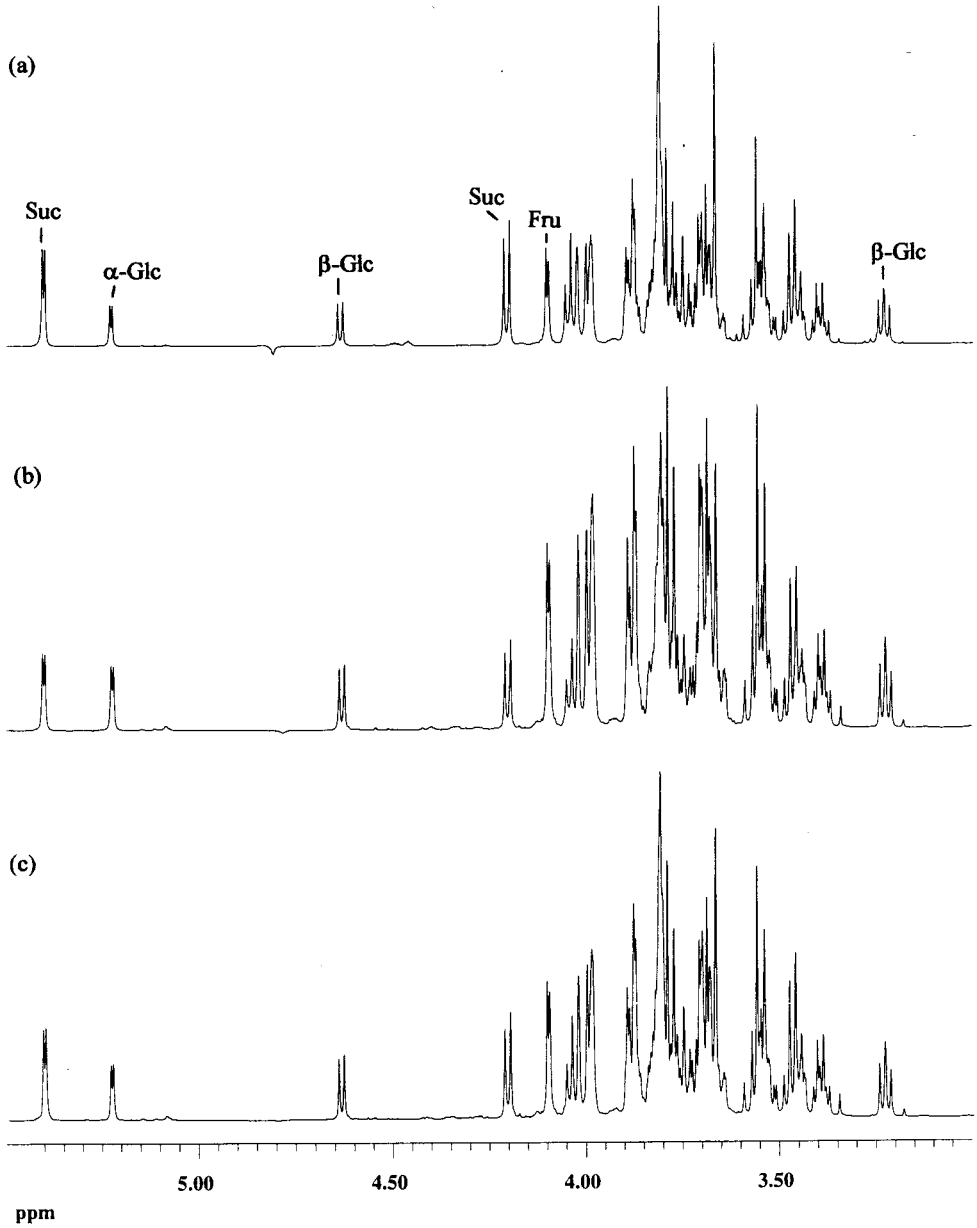

Figure 8. Expansions of the 3.0−5.5 ppm regions of the 1D ^{1}H NMR spectra of juices of (a) day 1, (b) day 15, and (c) day 19.

day 19 results from an error in the evaluation of the area under the 5.23 ppm peak. The peak sits on a broad band from incomplete water suppression so that a true baseline is not obtained: observation of the β-Glc H2 signal (3.25 ppm) shows that no such increase occurs.

The proportion of the main sugars in the juices were measured from the corresponding high resolution NMR spectra in the same way as described for the pulps, and the results are also presented in Table 2. Those results show considerable discrepancies relative to the pulps and previously reported results obtained by HPLC. First, the percentage of sucrose is seen by NMR to be significantly lower (apart from day 1) than values found here for the pulps or previously reported, while glucose and fructose levels are significantly higher. This suggests that sucrose hydrolysis may have occurred to some extent before the juice spectra were recorded. Indeed, this is likely to happen if the stored juices are not characterized immediately after having been thawed. In fact, the NMR spectra of the juices were recorded 1 or 2 days after thawing during which time the samples were kept at 4 °C. These conditions may have allowed sucrose hydrolysis to proceed to some extent. On the other hand, since the pulp spectra were run immediately after thawing, the corresponding sugar compositions do not reflect extensive sucrose hydrolysis. These results confirm the importance of carrying out mango juice analysis immediately after the juices are obtained, either directly from the fruit or as soon as possible after thawing.

The NMR spectra of both pulps and juices may, in principle, enable the relative amounts of α-glucose and β-glucose to be estimated by measuring the areas of the α-anomer peak at 5.23 ppm and the β-H2 peak at 3.25 ppm. This is, to our knowledge, the first time that the two anomeric glucose forms have been estimated as a function of the ripening of mango. Table 2 shows that the α/β ratio found for the juice spectra is close to that expected in aqueous solution—0.61 at 31 °C (Angyal, 1984)—although, interestingly, the initial stage of ripening seems to be characterized by a slightly lower ratio (0.51 compared to 0.61). The values obtained for the

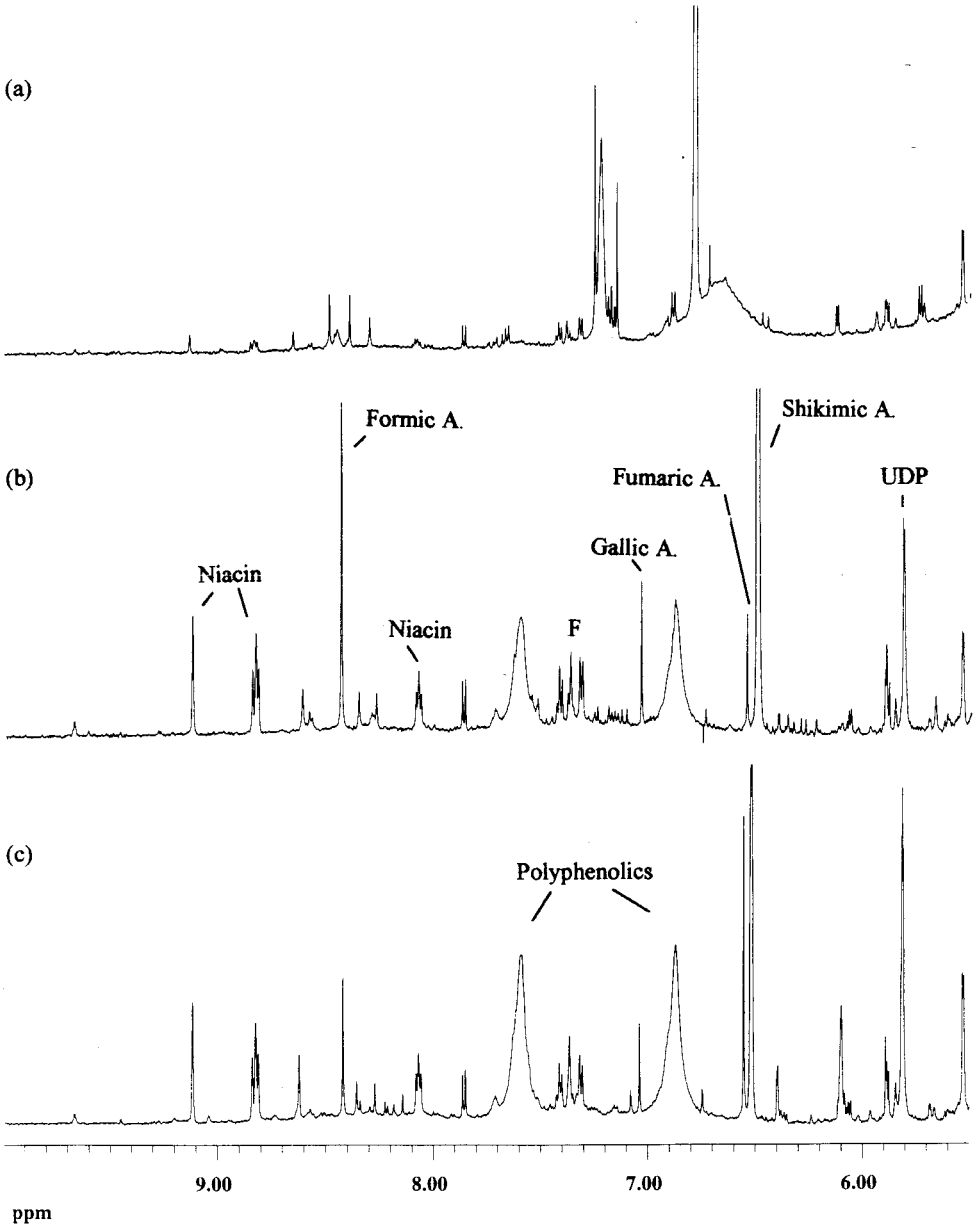

Figure 9. Expansions of the 5.5−10.0 ppm regions of the 1D ^{1}H NMR spectra of juices of (a) day 1, (b) day 15, and (c) day 19.

pulps are significantly different in that they show, for most ripening stages, a ratio of ca. 0.36. However, this observation must be interpreted with care since a possible underestimation of the α-anomer area may arise, due to off-resonance effects of water saturation. This point requires further investigation in order to optimize the estimation of glucose anomers in pulps, and its results will be reported in a subsequent communication.

Ratios of Citric Acid and Alanine to Total Sugars. The ratio of the area under the citric acid multiplets at 2.80−2.95 ppm to the total area under the sugar peaks may be converted into molar ratio of citric acid/total sugars. The resulting molar ratios are given in Table 3 for the pulps collected for days 1 and 5 and for the juice collected for day 1. The marked decrease of citric acid noted after day 5 prevented its spectral integral from being measured for the later stages of ripening. The values obtained are of the same order of magnitude as those reported in the literature (Medlicott et al., 1986) for days 3 and 6. The slightly overestimated values may result from the partial overlap of the citric acid peaks with those of malic acid. This is consistent with the reported decrease in citric acid to about 0.6 mequiv per 100 g of fresh weight, after 15 days ripening (Medlicott et al., 1986). For such low concentrations, the measurement of the resulting NMR intensity is severely hindered by overlap with peaks of comparable intensities arising for instance from malic acid (Table 1).

Table 3 also shows the alanine/total sugars ratio obtained by integration of the alanine doublet at 1.47 ppm. It is clear from such values that the ripening process is accompanied by a significant increase of alanine relative to total sugars. The values recorded here are in broad agreement with those found in the literature for different varieties of mangoes of unspecified maturity (Fang and Ghang, 1980, 1981). Since the amount of total sugars is known to increase as mango ripens (Medlicott and Thompson, 1984; Medlicott et al., 1986; Selvaraj et al., 1989; Castrillo et al., 1992; Ito et al., 1997), this result reflects an absolute increase for alanine which is, in the pulps, almost five times more

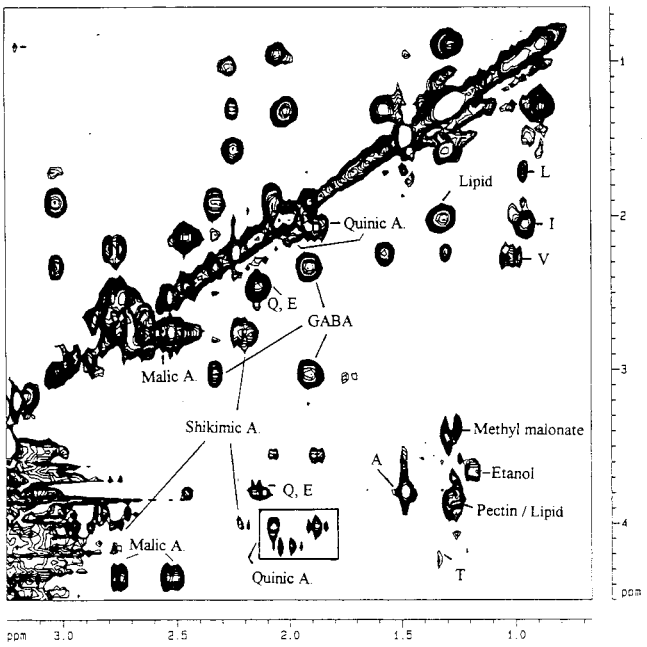

Figure 10. Expansion of the aliphatic region of the TOCSY spectrum obtained for the pulp of day 19 (see Table 1 for complete assignment).

marked than that for the sugars. The values registered for the juices suggest an enhanced increase of alanine, reflecting some differences observed between the values found for juices and pulps. The full interpretation of these differences requires a more comprehensive comparative investigation, which must also take into account the influence of sample history. These aspects will be the subject of a later communication. At this stage, only the clear increase of alanine with ripening will be discussed. The significant increase of alanine, compared to other aliphatic amino acids (multiplets at 0.94−1.3 ppm), suggests that a separate biosynthetic process may exist for alanine, probably involving a link between pyruvic acid (or pyruvate) and alanine.

Ripening-Related Changes of Minor Peaks. The changes observed during ripening for the less intense signals in the 0−3.0 and 5.5−10.0 ppm regions of the spectra of pulps and juices will now be discussed. The isoleucine, valine, and leucine aliphatic peaks all increase with ripening which is indicative of a possible common biosynthetic path for those amino acids. The peak at 1.12 ppm, possibly due to β-carotene, is absent or very weak in day 1 (Figures 4a and 7a), but it increases slightly during ripening (Figures 4c and 7c). β-Carotene, the most abundant carotenoid in mango, has indeed been found to increase in the 2.0−5.8 μg/g range, during the ripening of "Tommy Atkins" mangoes (Mercadante and Rodriguez-Amaya, 1998). On the downfield side of the broad 1.25−1.30 ppm peak observed for the pulps, some signals become more noticeable upon ripening suggesting an increase in lactate, as clearly observed in the juices (Figure 7). In the 1.5−1.8 ppm region, the arginine multiplet is clearly seen for day 1 juice and partially defined for the pulp. At days 15 and 19, this multiplet is replaced by a new and weaker set of peaks which may be assigned to ornithine or lysine (Table 1; Figures 4d and 7b). Although the assignment of such peaks to ornithine is not completely definite (see Table 1), the appearance of this compound in ripe mango together with the disappearance of arginine suggests that, since the two compounds are chemically related, some kind of biosynthetic path may exist between them. In support of this, it is noted that in fruits such as plum, cherry, and nectarine which contain significant quantities of ornithine, the arginine content is particularly low (Van Gorsel et al., 1992) whereas grapefruit has been found to contain measurable quantities of arginine but only traces of ornithine (Wallrauch, 1981). Further downfield, the 2.01 ppm singlet present for day 19 juice (Figure 7c) is absent or very weak in all the pulps spectra; this peak may arise from a soluble flavor component, such as ethyl acetate, developing at later ripening stages, but at this stage a more objective assignment is not possible. The GABA peaks at 1.90, 2.33, and 3.01 ppm, practically absent in day 1, clearly increase during ripening (Figures 4 and 7). Finally, the increase of the 2.53 ppm peak, compared to malic acid (multiplet at 2.7 ppm) suggests that ripening is accompanied by an increase in succinic acid and/or methylamine, relative to malic acid.

In the aromatic region of the pulps' spectra (Figure 6), the resolution is significantly lower than in the juices spectra (Figure 9); however, most of the peaks identified in the latter become more resolved in the spectra of ripened pulps. The aromatic spectra of day 1 show a dominance of the shikimic acid peak at 6.79 ppm, shifted to lower field by the lower pH of unripe mango, and of the broad features at 6.69 and 7.23 ppm (both arising from arginine) which disappear with ripening. Narrower and weaker resonances are observable showing that relatively small amounts of other metabolites (e.g., niacin, phenylalanine, and UDP) occur in the early ripening stages (Figures 6a and 9a). As ripening proceeds, significant changes occur in the chemical shift and intensity of the broad bands, as observed in Figure 6a−d. At the final stage of ripening (day 19), the pulp spectrum is very similar to that of the corresponding juice, showing two broad peaks at 6.25−6.5 ppm and 6.9−7.0 ppm which arise from polyphenolic compounds formed during ripening. Since the peaks of formic acid, gallic acid, and shikimic acid decrease in the juice spectrum (Figure 9c), compared to those broad peaks, it may be suggested that such compounds may act as precursors in the polymerization process. Moreover, the doublet centered at 7.14 ppm, possibly arising from tyrosine, decreases from day 15 to day 19, while the amount of phenylalanine increases. Whereas tyrosine may be involved in the biosynthesis of polymeric moieties, phenylalanine does not seem to be significantly used up since its content increases, probably in connection with the decrease of its precursor shikimic acid.

In summary, this work shows that standard MAS enables resolved NMR spectra of intact mango pulp to be recorded but HR-MAS results in a much more marked resolution improvement, making possible the use of efficient water suppression and two-dimensional NMR. This enables the overall biochemistry of the fruit to be studied noninvasively. In this work, just under 40 metabolites other than the main sugars were identified in mango samples at different ripening stages. In pulps, sucrose predominates over fructose and glucose at most ripening stages, and the variation of each sugar with ripening was in broad agreement with that reported previously for mango juice. In the juices, the sugar composition and its variation with ripening differed significantly from that reported previously, and the possibility of some sucrose hydrolysis occurring after

Table 1. ^{1}H and ^{13}C NMR Assignments of Mango Pulps and Juices[a]

compound	chemical shift (ppm): multiplicity: *J* (Hz)					
acetaldehyde hydrate	1.32	5.25				
adenine	8.27:s	8.61:s				
alanine (A)	1.47:d:7.4	3.77:m				
	17.22	51.53				
γ-aminobutyric acid	1.90:m	2.33:t:7.6	3.01:t:7.6			
	24.35	34.70	40.21			
arginine[b] (R)	1.59−1.77	1.91	3.25	6.66	7.23	
asparagine (N)	2.85:dd:7.6, 16	2.95:dd:4, 16	4.01			
	35.51	35.51				
aspartic acid (D)	2.69:dd:9.6, 16	2.83:dd:3.6, 1	3.92			
	37.29	37.29				
β-arabinose	3.49	4.57				
3OH-butyric acid	1.20	4.19				
β-carotene[c]	1.12	1.98				
	19.33					
choline	3.18					
	54.77					
citric acid[b]	2.77:d	2.91:d				
	45.22	45.22				
ethanol	1.17:t:7.4	3.65				
formic acid	8.45					
fructose	4.11:m					
β-fucose[c]	1.25	3.78				
	17.38					
fumaric acid	6.55					
β-galactose[c]	3.49	4.57				
gallic acid	7.04					
α-glucose	5.23:d					
β-glucose	3.25:dd	4.64:d				
glutamine (Q)/glutamic acid (E)	2.13:dd:7, 15	2.45:dd:7, 15	3.77			
	27.09	31.79	55.09			
isoleucine (I)	0.94:m	1.00:d:6.8	1.26:m	1.47:m		
		15.60	15.60	19.16		
lactate	1.33	4.12				
	20.95	69.01				
leucine	0.95:m	1.71:m				
	22.89					
lysine	1.61	1.71	3.01			
malic acid	2.51	2.75	4.33			
methanol	3.35					
	49.92					
methylamine[c]	2.53					
	32.27					
methyl malonate	1.30	3.42				
niacin	8.08:dd:8, 8	8.83:dd:8, 8	9.12			
ornithine[c]	1.65−1.77					
phenylalanine (F)	3.13	3.49	3.81	7.31	7.37	7.43
	43.31	43.31	53.80			
polyphenols	6.88	7.61				
quinic acid	1.87:dd	2.07:m	4.02	1.96:m	2.04:m	4.14
	41.50	41.50		38.26	38.26	
β-rhamnose	1.28	3.88				
	17.54					
shikimic acid	2.19	2.75	3.71	3.99	4.40	6.51
	33.08	33.08	76.78	68.21	67.07	132.30
succinic acid[c]	2.53					
sucrose	4.22:d	5.40:d				
tartaric acid	4.43					
	78.89					
threonine (T)	1.32	4.25				
	29.20					
valine (V)	0.98:d:6.8	1.04:d:6.8	2.27	3.60		
	17.55	18.84	29.85			

[a] Unless otherwise indicated the pH dependent chemical shifts of organic acids are indicated for day 15. ^{13}C chemical shifts are indicated (where available from H/C correlation spectrum) in a second row below the correlated ^{1}H chemical shift. Coupling constants (*J*) were measured in hertz at 600 MHz field strength. s: singlet, m: multiplet, d: doublet, t: triplet, dd: doublet of doublets. [b]Chemical shift values refer to day 1 (pH ≅ 3.5). [c]Possible assignment.

preparation of the samples is suggested. Citric acid is confirmed to be the most abundant organic acid in unripe mango, decreasing abruptly after the initial stages of ripening. Ripening is accompanied by a significant increase in alanine and lesser increases in lactate, GABA, phenylalanine, and niacin. Marked changes in the aromatic spectral region of the pulps reflect the complex chemistry of polyphenolic compounds and suggest the possible role of formic acid, gallic acid, shikimic acid, and tyrosine as precursors.

Table 2. Proportions of the Main Sugars Found in Mango and Their Dependence upon Ripening

	sucrose	fructose	glucose	α-glu	β-glu	α/β-glu	glu/fru
			Juices				
day 1	40.8	34.6	24.6	16.3	8.3	0.51	0.71
day 15	21.2	53.3	25.5	16.3	9.2	0.56	0.48
day 19	31.2	43.5	25.4	15.8	9.5	0.60	0.58
			Pulps				
day 1	41.3	38.2	20.4	15.0	5.4	0.36	0.53
day 5	43.3	49.3	7.5	5.5	2.0	0.36	0.15
day 15	51.1	42.0	6.9	5.0	1.9	0.38	0.16
day 19	53.0	34.1	12.9[a]	7.9[a]	5.0	0.63[a]	0.38[a]
			Published[b]				
day 3	57.1	27.5	15.5				0.56
day 6	54.4	40.2	5.5				0.14
day 9	69.9	30.2	0				0
day 11	65.9	30.5	3.6				0.12
day 15	73.2	26.8	0				0

[a] Overestimated values due to the broad signal overlapping the α-glucose peak at 5.23 ppm. [b] Calculated from values published for juices (Medlicott et al., 1986).

Table 3. Molar Ratios Obtained from the ^{1}H HR-MAS NMR Spectra of Mango Pulps and Mango Juices during Ripening (T: Total Sugars)

	this work				published				
ratio	day 1	day 5	day 15	day 19	day 3	day 6	day 9	day 11	day 15
					Juices				
citric acid/T	0.138		*a*	*a*	0.064[b]	0.071[b]	0.0048[b]	0.0147[b]	0.0068[b]
alanine/T	0.0018		0.0125	0.0160		0.0086,[c] 0.00145[c]			
					Pulps				
citric acid/T	0.109	0.082	*a*	*a*					
alanine/T	0.0039	0.0056	0.0088	0.0183					

[a] Citric acid signal is too weak to be integrated. [b] From Medlicott et al., 1986. [c] Calculated from values published for cultivars Keitt and Irwin and in unspecified ripening stages (Fang and Ghang, 1980; Fang and Ghang, 1981).

ACKNOWLEDGMENT

The authors thank P. Belton for useful discussions and B. Goodfellow for contributing to the spectral assignment performed in this work. I. Duarte thanks the University of Aveiro for partial funding of this work and PRAXIS XXI for the grant BD/15666/98. I.J. Colquhoun thanks the BBSRC for support through the Competititve Strategic Grant.

LITERATURE CITED

Aina, J. O.; Oladunjoye, O. O. Respiration, pectolytic activity and textural changes in ripening african mango (Irvingia gabonensis) fruits. *J. Sci. Food Agric.* **1993**, *63*, 451−454.

Angyal, S. J. The composition of reducing sugars in solution. *Adv. Carbohydr. Chem. Biochem.* **1984**, *42*, 15−65.

Belton, P. S.; Delgadillo, I.; Gil, A. M.; Casuscelli, F.; Colquhoun, I. J.; Dennis, M. J.; Spraul, M. High field proton NMR studies of apple juices. *Magn. Reson. Chem.* **1997**, *35*, S52−S60.

Belton, P. S.; Delgadillo, I.; Holmes, E.; Nicholls, A.; Nicholson, J. K.; Spraul, M. Use of high-field ^{1}H NMR spectroscopy for the analysis of liquid foods. *J. Agric. Food Chem.* **1996**, *44*, 1483−1487.

Belton, P. S.; Gil, A. M. Magic angle spinning spectra of rare and abundant nuclei in food materials. *J. NMR Anal.* **1996**, *2*, 45−52.

Bhushan, B.; Kadam, R. M.; Thomas, P.; Singh, B. Evaluation of electron spin resonance technique for the detection of irradiated mango. *Int. J. Food Sci. Technol.* **1994**, *29*, 679−686.

Bustos, M. E.; Romero, M. E.; Gutierrez, A.; Azorin, J. Identification of irradiated mangoes by means of ESR spectroscopy. *Appl. Radiat. Isot.* **1996**, *47*, 1655−1656.

Cano, M. P.; Ancos, B. Carotenoid and carotenoid ester composition in mango fruit as influenced by processing method. *J. Agric. Food Chem.* **1994**, *42*, 2737−2742.

Castrillo, M.; Kruger, N. J.; Whatley, F. R. Sucrose metabolism in mango fruit during ripening. *Plant Sci.* **1992**, *84*, 45−51.

Chassagne, D.; Crouzet, J. Free and bound volatile components of temperate and tropical fruits. *ACS Symp. Ser.* **1995**, *596*, 182−189.

Colquhoun, I. J. High-resolution NMR spectroscopy in food analysis and authentication. *Spectrosc. Eur.* **1998**, *10*, 8−18.

Eads, T. M.; Bryant, R. G. High-resolution proton NMR spectroscopy of milk, orange juice, and apple juice with efficient supression of the water peak. *J. Agric. Food Chem.* **1986**, *34*, 834−837.

Engel, K. H.; Tressl, R. Studies on the volatile components of two mango varieties. *J. Agric. Food Chem.* **1983**, *31*, 769−801.

Fan, T. W.-M. Metabolite profiling by one- and two-dimensional NMR analysis of complex mixtures. *Prog. Nucl. Magn. Reson. Spectrosc.* **1996**, *28*, 161−219.

Fang, T. T.; Ghang, K. J. Standardisation on the inspection of natural fruit juice 1. Profile analysis of free amino acids in some natural fruit juices. *Mem. Coll. Agric. Nat.* **1980**, *20*, 74−82.

Fang, T. T.; Ghang, K. J. Standardisation on the inspection of natural fruit juice 3. Determination of sugar pattern of natural fruit juice. *Mem. Coll. Agric. Nat.* **1981**, *21*, 62−69.

Gil, A. M.; Alberti, E.; Belton, P. S.; Humpfer, E.; Spraul, M. A magic angle spinning NMR study of the wheat storage protein omega-gliadins. *Magn. Res. Chem.* **1997**, *35*, S101−S111.

Gil, A. M.; Belton, P. S.; Hills, B. Applications of NMR to Food Science. In *Annual Reports in NMR Spectroscopy*; Academic Press Ltd.: London, 1996.

Guthrie, J.; Walsh, K. Noninvasive assessment of pineapple and mango fruit quality using near infrared spectroscopy. *Aust. J. Exp. Agric.* **1997**, *37*, 253−263.

Ito, T.; Sasaki, K.; Yoshida, Y. Changes in respiration rate, saccharide and organic acid content during development and

ripening of mango fruit (Mangifera indica L. 'Irwin') cultured in a plastic house. *J. Jpn. Soc. Hortic. Sci.* **1997**, *66*, 629−635.

Joyce, D. C.; Hockings, P. D.; Mazucco, R. A.; Shorter, A. J.; Brereton, I. M. Heat treatment injury of mango fruit revealed by nondestructive magnetic resonance imaging. *Postharv. Biol. Technol.* **1993**, *3*, 305−311.

Koulibaly, A.; Sakho, M.; Crouzet, J. Variability of free and bound volatile terpenic compounds in mango. *Lebensm.-Wiss. Technol.* **1992**, *25*, 374−379.

Malundo, T. M. M.; Baldwin, E. A.; Moshonas, M. G.; Baker, R. A.; Shewfelt, R. L. Method for the rapid headspace analysis of mango homogenate volatile constituents and factors affecting quantitative results. *J. Agric. Food Chem.* **1997**, *45*, 2187−2194.

Medlicott, A. P.; Reynolds, S. B.; Thompson, A. K. Effects of temperature on the ripening of mango fruit (Mangifera indica L. var Tommy Atkins). *J. Sci. Food Agric.* **1986**, *37*, 469−474.

Medlicott, A. P.; Thompson, A. K. Analysis of sugars and organic acids in ripening mango fruits (Mangifera indica L. var Keitt) by high performance liquid chromatography. *J. Sci. Food Agric.* **1984**, *36*, 561−566.

Mercadante, A. Z.; Rodriguez-Amaya, D. B. Effects of ripening, cultivar differences, and processing on the carotenoid composition of mango. *J. Agric. Food Chem.* **1998**, *46*, 128−130.

Mercadante, A. Z.; Rodriguez-Amaya, D. B.; Britton, G. HPLC and mass spectrometric analysis of carotenoids from mango. *J. Agric. Food Chem.* **1997**, *45*, 120−123.

Mitcham, E. J.; McDonald, R. E. Cell wall modification during ripening of Keitt and Tommy Atkins mango fruit. *J. Am. Soc. Hortic. Sci.* **1992**, *117*, 919−924.

Mizrach, A.; Flitsanov, U.; Fuchs, Y. An ultrasonic nondestructive method for measuring maturity of mango fruit. *Trans. ASAE* **1997**, *40*, 1107−1111.

Muda, P.; Seymour, G. B.; Errington, N.; Tucker, G. A. Compositional changes in cell wall polymers during mango fruit ripening. *Carbohydr. Polym.* **1995**, *26*, 255−260.

Ni, Q. W.; Eads, T. M. Low-Speed Magic-Angle-Spinning Carbon-13 NMR of Fruit Tissue. *J. Agric. Food Chem.* **1992**, *40*, 1507−1513.

Ni, Q. W.; Eads, T. M. Liquid-phase composition of intact fruit tissue measured by high-resolution proton NMR. *J. Agric. Food Chem.* **1993a**, *41*, 1026−1034.

Ni, Q. W.; Eads, T. M. Analysis by proton NMR of changes in liquid-phase and solid-phase components during ripening of banana. *J. Agric. Food Chem.* **1993b**, *41*, 1035−1040.

Nicholson, J. K.; Foxall, P. J. D.; Spraul, M.; Farrant, D.; Lindon, J. C. 750 MHz ^{1}H and ^{1}H-^{13}C NMR spectroscopy of human blood plasma. *Anal. Chem.* **1995**, *67*, 793−811.

Ollé, D.; Baumes, R. L.; Bayonove, C. L.; Lozano, Y. F.; Sznaper, C.; Brillouet, D. M. Comparison of freee and glicosidically linked volatile components from polyembrionic and monoembryonic mango (Mangifera indica L.) cultivars. *J. Agric Food Chem.* **1998**, *46*, 1094−1110.

Ollé, D.; Lozano, Y. F.; Brillouet, J. M. Isolation and characterisation of soluble polysaccharides and insoluble cell wall material of the pulp from four mango (Mangifera indica L.) cultivars. *J. Agric. Food Chem.* **1996**, *44*, 2658−2662.

Sakho, M.; Chassagne, J.; Crouzet, J. African mango glicosidically bound volatile compounds. *J. Agric. Food Chem.* **1997**, *45*, 883−888.

Salunkhe D. K.; Desai, B. B. Mango. In *Postharvest Biotechnology of Fruits*; CRC Press: London, 1984.

Selvaraj, Y.; Kumar, R.; Pal, D. K. Changes in sugars, organic acids, amino acids, lipid constituents and aroma characteristics of ripening mango (Mangifera indica L) fruit. *J. Food Sci. Technol.* **1989**, *26*, 308−313.

Sudhakar, D. V.; Maini, S. B. Stability of carotenoids during storage of mango pulp. *J. Food Sci. Technol.* **1994**, *31*, 228−230.

Thomas, P.; Saxena, S. C.; Chandra, R.; Rao, R.; Bhatia, C. R. X-ray imaging for detecting spongy tissue, an internal disorder in fruits of Alphonso mango (Mangifera indica L.). *J. Hortic. Sci.* **1993**, *68*, 803−806.

Tucker, G. A.; Seymour, G. B. Cell wall degradation during mango fruit ripening. *Acta Hortic.* **1991**, *291*, 454−460.

Usha, K.; Gambhir, P. N.; Sharma, H. C.; Goswami, A. M.; Singh, B. Relationship of molecular mobility of water with floral malformation in mango as assessed by Nuclear Magnetic Resonance. *Sci. Hortic.* **1994**, *59*, 291−295.

Usha, K.; Goswami, A. M.; Sharma, H. C.; Singh, B.; Pande, P. C. Scanning electron microscopic studies on floral malformation in mango. *Sci. Hortic.* **1997**, *71*, 127−130.

Van Gorsel, H.; Li, C.; Kerbel, E. L.; Smits, M.; Kader, A. A. Compositional characterization of prune juice. *J. Agric. Food Chem.* **1992**, *40*, 784−789.

Wallrauch, S. Beitrag ueber die Zusammensetzung israelischer grapefruitsaefte. *Fluessiges Obst.* **1981**, *4a*, 197−202.

Wilberg, V. C.; Rodriguez-Amaya, D. B. HPLC quantitation of major carotenoids of fresh and processed guava, mango and papaya. *Lebensm.-Wiss. Technol.* **1995**, *28*, 474−480.

Received for review October 18, 1999. Revised manuscript received February 4, 2000. Accepted February 7, 2000.

JF9911287